Video Article

Multimodal Optical Microscopy Methods Reveal Polyp Tissue Morphology and Structure in Caribbean Reef Building Corals

Mayandi Sivaguru[1], Glenn A. Fried[1], Carly A. H. Miller[1,2], Bruce W. Fouke[1,2,3]

[1]Institute for Genomic Biology, University of Illinois at Urbana-Champaign

[2]Department of Geology, University of Illinois at Urbana-Champaign

[3]Department of Microbiology, University of Illinois at Urbana-Champaign

Correspondence to: Mayandi Sivaguru at sivaguru@illinois.edu, Bruce W. Fouke at fouke@illinois.edu

URL: http://www.jove.com/video/51824
DOI: doi:10.3791/51824

Keywords: Environmental Sciences, Issue 91, Serial block face imaging, two-photon fluorescence microscopy, *Montastraea annularis*, *Montastraea faveolata*, 3D coral tissue morphology and structure, zooxanthellae, chromatophore, autofluorescence, light harvesting optimization, environmental change

Date Published: 9/5/2014

Citation: Sivaguru, M., Fried, G.A., Miller, C.A.H., Fouke, B.W. Multimodal Optical Microscopy Methods Reveal Polyp Tissue Morphology and Structure in Caribbean Reef Building Corals. *J. Vis. Exp.* (91), e51824, doi:10.3791/51824 (2014).

Abstract

An integrated suite of imaging techniques has been applied to determine the three-dimensional (3D) morphology and cellular structure of polyp tissues comprising the Caribbean reef building corals *Montastraeaannularis* and *M. faveolata*. These approaches include fluorescence microscopy (FM), serial block face imaging (SBFI), and two-photon confocal laser scanning microscopy (TPLSM). SBFI provides deep tissue imaging after physical sectioning; it details the tissue surface texture and 3D visualization to tissue depths of more than 2 mm. Complementary FM and TPLSM yield ultra-high resolution images of tissue cellular structure. Results have: (1) identified previously unreported lobate tissue morphologies on the outer wall of individual coral polyps and (2) created the first surface maps of the 3D distribution and tissue density of chromatophores and algae-like dinoflagellate *zooxanthellae* endosymbionts. Spectral absorption peaks of 500 nm and 675 nm, respectively, suggest that *M. annularis* and *M. faveolata* contain similar types of chlorophyll and chromatophores. However, *M. annularis* and *M. faveolata* exhibit significant differences in the tissue density and 3D distribution of these key cellular components. This study focusing on imaging methods indicates that SBFI is extremely useful for analysis of large mm-scale samples of decalcified coral tissues. Complimentary FM and TPLSM reveal subtle submillimeter scale changes in cellular distribution and density in nondecalcified coral tissue samples. The TPLSM technique affords: (1) minimally invasive sample preparation, (2) superior optical sectioning ability, and (3) minimal light absorption and scattering, while still permitting deep tissue imaging.

Video Link

The video component of this article can be found at http://www.jove.com/video/51824/

Introduction

Global warming and accompanying environmental change are directly affecting the health and distribution of tropical marine corals[1-4]. Multiple impacts are being observed, including coral bleaching and the emergence of infectious diseases[5-6]. However, more accurate prediction of future coral response to these environmental threats will require that a histological “baseline” be established, which defines tissue morphology and cell composition and distribution for “apparently healthy” corals. In turn, “impacted” corals can then be quantitatively compared. Furthermore, this baseline should be established for apparently healthy corals under a variety of environmental conditions, so that “healthy response” can also be gauged across environmental gradients. As an initial step toward establishing this baseline, a high-resolution 3D study has been undertaken of how apparently healthy coral polyp tissue morphology and cellular composition responds to increases in water depth (WD) and accompanying decreases in sunlight irradiance. Results can then be used to establish a more comprehensive mechanistic understanding of coral adaptation, as well as to gain insight into coral-symbiont evolution and the enhancement of light harvesting.

Stony corals (*Scleractinia*) are colonial marine invertebrate animals that play host to a complex assemblage of other microorganisms, collectively referred to as the *coral holobiont*[7-10]. The research undertaken in the present study seeks to use a suite of cutting-edge imaging technologies to simultaneously track changes with increasing water depth in the tissue pigments and symbiotic zooxanthellae of apparently healthy host corals. This will establish the required comparative tissue cell “baseline” across a bathymetric gradient for apparently healthy corals and act as indicators of coral health[10]. Coral pigments, called *chromatophores*, act to absorb, reflect, scatter, refract, diffract, or otherwise interfere with incident solar radiation[11]. The zooxanthellae-chromatophore endosymbiotic relationship has enabled the coevolution of strategically advantageous light-harvesting optimization and skeletal growth strategies, as well as trophic plasticity (shifting feeding strategies back-and-forth from autotrophy to heterotrophy) for the coral animal[12].

The southern Caribbean island nation of Curaçao (formerly part of the Netherlands Antilles) lies approximately 65 km north of Venezuela within the east-west trending Aruba-La Blanquilla archipelago (**Figure 1A**). The 70 km long southern coast of Curaçao contains a continuous modern and Miocene-Pliocene-Pleistocene-Holocene ancient fringing coral reef tract[13,14]. Mean annual SST on Curaçao varies approximately 3 °C

annually, ranging from a minimum of 26 °C in late January to a maximum of 29 °C in early September, with a mean annual temperature of 27.5±0.5 ºC (NOAA SST Data Sets, 2000-2010). The coral reef at Playa Kalki (12°22'31.63"N, 69°09'29.62"W), lying near the northwestern tip of Curaçao (**Figure 1A**), was chosen for sampling because it has been previously well-studied and the marine ecosystem at this location is bathed in fresh nonpolluted seawater[7,15-19]. Two closely related scleractinian coral species, *M. annularis* and *M. faveolata*, were chosen for experimentation and analysis in this study because each species: (1) exhibits distinctly different and nonoverlapping bathymetric distributions on the reef tract with respect to the shelf break and the associated carbonate sedimentary depositional environments *(M. annularis* range = 0-10 m WD; *M. faveolata* range = 10-20 m WD[20]; **Figures 1B, 2A**, and **2B**); (2) is a common coral reef framework builder throughout the Caribbean Sea[21]; and (3) has well-studied ecological, physiological, and evolutionary relationships[22].

Field sampling for the present study was conducted using standard SCUBA diving techniques offshore of Playa Kalki on Curaçao. A shallow-to-deep water bathymetric transect was established that ran across the shelf, over the shelf break, and into the deep water fore reef environments. Apparently healthy coral heads were then identified for sampling along this bathymetric transect, including: (1) three individual ~ 1 m diameter coral heads of *M. annularis*, all of which were at 5 m water depth (WD); and (2) three individual ~ 1 m diameter coral heads of *M. faveolata*, all of which were at 12 m WD. Photosynthetically active radiation (PAR) was measured as 33-36% PAR at 5 m WD and 18-22% PAR at 10 m WD. Sampling was conducted in January when the SST was 26 °C at the water depths of both the 5 m and 12 m. Each of these six coral heads was sampled in triplicate at equivalent spatial positions (*i.e.*, approximately 45° N latitude on each of the six hemispherical coral heads). Each individual sample consisted of a 2.5 cm diameter coral tissue-skeleton core biopsy that was collected with a cleaned arch punch. Three coral tissue-skeleton biopsies were sampled on standard SCUBA with gloved hands from each of the coral heads (9 from *M. annularis* colonies at 5 m WD and 9 from *M. faveolata* at 12 m WD). Immediately upon collection at depth, each biopsy core sample was placed in a sterile 50 ml polypropylene centrifuge tube, screw-top sealed, and returned to the surface. The seawater was decanted from each centrifuge tube and each core biopsy was then immersed, stored, and transported in 4% paraformaldehyde.

SBFI imaging has previously been performed on a wide range of biological samples, including whole-brain and whole-heart human tissues, intact mouse embryos, zebra fish embryos, and multiple types of animal samples with intact bones[23-30]. Most of these studies utilized optical/light microscopy with either fluorescence or bright field techniques. However, studies have been conducted at ultra-high magnifications using scanning electron serial block face imaging in the past[31]. In the present study, a modified SBFI protocol has been developed for and applied to corals for the first time. Because *M. annularis* and *M. faveolata* coral polyps are 1-2 mm in thickness, none of the routine light microscopy techniques would be capable of penetrating the entire thickness of coral polyp tissue. Therefore, we have SBFI sample preparation protocol specifically designed for coral samples. In addition, we have custom designed a stereomicroscope holder, which is motorized to move in both x and y directions. This apparatus takes images of the block face of the sample rather than collecting the sections using a regular microtome in front of the microscope. We also introduced another nonlinear optical two-photon microscopic technique to image the same coral polyps across the entire thickness of the coral tissues. This overcomes the limitations imposed by SBFI in terms of decalcification and the possibility of changes in tissue morphology and volume (shrinking) that may be induced by sample preparation (dehydration) and processing protocols. Furthermore, the emission profiles from the corals were spectrally resolved to identify their peak emissions and variations between the chromatophores and the photosynthetic zooxanthellae. These results were evaluated in the context of the method used and their individual advantages regarding acquisition time, analysis time, and the ability to resolve fine structural details without compromising structural integrity of the coral tissue.

Protocol

NOTE: Reagents to be prepared for Serial Block Face Imaging of Coral Samples

1. Preinfiltration Wax

1. Melt 3.6 g of STEARIN flakes in a glass beaker. Mix well on a hot plate (60-70 °C).
2. Add 400 mg of Sudan IV (to minimize wax background fluorescence). Mix well and wait until a red translucent solution is achieved.
3. Add 96 ml hot molten paraffin (100%) and mix well.

1.2) Embedding Wax

1. Melt 7.2 g of STEARIN flakes in a glass beaker and mix well on a hot plate (60-70 °C).
2. Add 0.8 g of Sudan IV. Mix well and wait until a red translucent solution is achieved.
3. Add paraffin granules (162 g) and mix until paraffin melts completely.
4. Add 30 g of white granular Vybar and melt completely in the same beaker; once melted, mix.
5. Loosely close the glass bottle with a lid. Place the glass bottle in a 60 °C convection oven to keep the ingredients in a liquid state. Carry out all infiltrations in this oven.
6. Split the total volume of the 200 ml red wax in to two glass bottles of 100 ml each. Use one aliquot for infiltration and the other for final embedding.

1.3) Embedding Coral Tissues for Serial Block Face Imaging

1. Wash the coral polyps collected in the field (**SI Video 1**) and stored (3-6 months at 4-5 °C in paraformaldehyde) in phosphate buffered saline (3x 5 min) and decalcify when ready to be imaged. Decalcify the polyps in ExCal solution for 24 hr or until as the polyps are totally devoid of $CaCO_3$. Incubate several decalcified coral polyps as a single block in a 25, 50, 75, and 100% ethanol series, followed by 1x xylene substitute to dehydrate the samples.
2. Place the processed polyps in a preheated 65 °C oven containing 100% xylene substitute. Incubate for 30 min twice by changing to fresh solution. Orient the polyps in such a way that the top of the polyps faces down and the top surface is as flat as possible.
3. Make solutions of 2:1, 1:1, and 1:2 xylene substitute and preinfiltration wax (step 1.1) in 50 ml Falcon tubes.
4. Incubate coral polyps with these three increasing concentrations of preinfiltration wax, followed by 3x incubation in 100% preinfiltration wax for 30-60 min each time.

5. Note: Depending on the thickness of the samples, steps 1.3.1-1.3.5 could be increased with longer periods of time.
6. Move the samples to embedding wax (see step 1.2.6) after 3x incubation in 100% preinfiltration wax.
7. Remove the embedding wax after 30 min. Replace with fresh embedding wax and continue incubation for a minimum of 4 hr at 65 °C.

1.4) Embedding in Red Wax

1. Photograph the block (the stainless steel tray where the white wax is placed and on top of which the sample is placed). This is necessary because once embedded in the wax, the location of the sample will become invisible as the embedding red wax is opaque.
2. Place small drops of high melting point wax around the new preheated stainless steel embedding mold and allow it to cool. Pour a small volume of freshly melted embedding wax from second container as stated in step 1.2.6.
3. Position the coral polyp facing down quickly over the white wax dot, then place a plastic sample holder on the stainless steel tray and pour more embedding wax so that the wax comes up to the surface of the plastic mold.
4. Take the entire setup out of 65 °C oven and allow it to cool on a bench or a cool surface until the wax completely hardens.
5. This may take 6 hr up to day or two. Place the block desiccated in a refrigerator at 4 °C, protected from light, for long term storage.

1.5) Sectioning at the Serial Block Face Setup

1. Trim the block and cut 1 µm sections using a microtome. Do not collect the sections as they will become like powder. Remember, we are imaging only the block face. The sample appears when the white wax begins to disappear.
2. Capture images of the smooth block face which contains the sample every time a section is removed. Continue until the coral polyp disappears as in **SI Video 2**.
3. Record/Capture the images with a monochrome camera using a FITC fluorescent filter to pick up the auto-fluorescence of the chromatophores/coral polyp. Image 3-4 decalcified cores from each species.

2. Imaging Corals Under Two-photon Fluorescence Microscopy

1. Fix coral polyp cores, each containing around 10-12 polyps about an inch in diameter, in 4% paraformaldehyde at the site of collection (sea shore) as soon as they are harvested under water.
2. Keep samples at 4 °C until imaging. Washed cores are placed in the same solution upside down in a cover glass bottom dish (0.17 mm thick).
3. Using a two photon laser at 780 nm excitation, image 3-4 polyps at two different magnifications (digital zoom) using a 10X (0.3 NA) objective. The coral polyp shape and height varies between samples (usually 1-2 mm) and the imaging depth is also limited by the imaging objective's working distance.
4. Use the tile scan mode to collect approximately 25-100 (5 x 5 or 10 x 10 tiles) images per focal plane in xy and 50-100 images through the z axis at 10 or 20 µm interval, totaling around 5,000-10,000 images/coral polyp.
5. Image three to four polyp areas to represent a core and coral species. NOTE: Image acquisition time varies between 2-5 hr/polyp area.
6. Store all images in raw data format in the system's hard disk as LSM 5. Render 3D in a 3D image analysis and rendering software.

3. 3D Volume Rendering and Visualization of SBFI and Two-photon Spectral Fluorescence Data

1. Crop the 2D data to reduce the file size by focusing on a single polyp using the square cropping tool in the program and compile as a single tiff file (reduce the file size also by saving the file in 8 bit format) in the acquisition software.
2. Open the assembled files of the SBFI data (collected in step 1.5.1) or the tiled multiple z-stacks of two photon optical sections (collected in step 2.1.4) in the program Imaris Surpass module under volume algorithm.
3. Project the SBFI data rendered in 3D using a shadow projection. Create an isosurface mode where the voxels are thresholded to create a solid surface pattern (**SI Video 3**).
4. Visualize the 3D projections using a clipping plane algorithm at xy, xz, and yz orthogonal modes to reveal 3D structure and shape of corals.
5. Animate the projections using a key frame animation module in the same Imaris program (**SI Videos 3-7**).
6. Generate video files at 5% compression and generate a movie clips in avi format using volume (**SI Videos 4** and **6**), 3D and Isosurface modalities (**SI Videos 5** and **7**).

Representative Results

A custom designed SBFI apparatus (manufactured specifically for the present study; **Figure 3**) produced the first detailed 3D digital elevation maps (DEMs) of the outer surface texture and morphology of the *M. annularis* and *M. faveolature* coral polyps (**Figure 4** and **SI Videos 1-2**). This yielded images of previously undescribed stacked lobes of coral tissue concentrically radiating outward from the center of each polyp (**Figures 4B, 4D,** and **4E**). These lobes are stacked along the uppermost ridge of tissue-covered primary and secondary skeletal septa, with the radially outermost and lowermost elevation lobes eventually synthesizing and merging with coenosarc tissues between polyps. The 3D polyp shape and the associated lobes were well preserved despite the coral tissue sample having gone through several steps of high-temperature infiltration and embedding. The addition of Sudan dye successfully masked the background as opaque, with the black color having helped to maximize the contrast of each sample and increase the signal-to-noise ratio. 3D and orthogonal plane views showed the distribution of fluorescent components along the z-axis (**Figure 4B**). There were planes with wax flakes that sometimes obscured polyp surface detail, which were removed for clarity when creating projections. The major advantage of this technique is in revealing internal details of any thick sample, thus eliminating the need to take multiple sections and align them at a later time. Further, the images in this technique are already aligned when collected (**Figure 4A**), providing a z resolution of up to 1 µm from a sample size of up to 10 mm or more (depending on the total drive distance of

the block holder in the microtome). It is possible to discriminate different auto-fluorescent components (using multiple filters) as well as individual zooxanthellae at higher magnification, provided the reduced field of view is acceptable.

The ApoTome optical sectioning fluorescence microscope revealed the distribution of coral tissues cells (zooxanthellae and chromatophores) and surface tissue structure at a submillimeter resolution. Hence, the 6-13 µm diameter zooxanthellae could be easily recognized and quantified with respect to number of cells per tissue volume (**Figure 5**). The dual channel image acquisition using the chlorophyll fluorescence (green) and the mucus labeled with WGB Alexa 647 (shown in red), worked best to quantify the level of mucus and the number of zooxanthellae within a given location of the polyp (major and minor septa of polyp could be calculated independently).

In addition to these microscope approaches, we have also applied TPLSM, a nonlinear technique widely used for thick biological samples. The major advantages of TPLSM over one-photon continuous wave lasers are that: (1) excitation occurs only at the point of focus because the power of the excitation light intensity becomes squared and the chance of a molecule to absorb two consecutive photons to excite one electron from the fluorophore is limited to the depth of field of the objective, thus providing an inherent confocality. and (2) as a consequence there will be no loss of an excitation photon while penetrating deeper into the sample, as opposed to single photon lasers. In addition, most biological tissue samples also absorb visible light. Since the two-photon excitation is inherently long (in near infrared at 780 nm), the absorption is also substantially minimized. On the other hand, the coral skeleton composed of calcium carbonate barely absorbs or scatters the two-photon light. Finally, since we were interested in determining the distribution of objects only on the contoured surface of the coral skeleton, we found deeper imaging using this modality very suitable for coral imaging.

We have attempted to characterize the available spectral signatures in *M. annularis* (**Figures 6-9**). Here we show that under the 780 nm two-photon excitation, the chromatophore auto-fluorescence has a peak around 500 nm, while the chlorophyll fluorescence from zooxanthellae is centered at approximately 675 nm (**Figure 6**). While unmixing of this spectral data (**Figures 6-7**) is also possible with an unmixing algorithm in the software (**Figure 8**), since there is a clear spectral distance between the two components, imaging them simultaneously using two detectors at two emission bands proved to be most time saving technique. This is especially true when the sample is tiled and imaged over an entire 1-2 mm depth of tissue. This eliminates the need for physical sectioning, which requires several thousand images per location and sample and polyp. The distribution of auto-fluorescent chromatophores is also distinct (**Figure 9**) among the two coral species tested. In one case, we observed a significant increase of chromatophores in the shallower-water dwelling coral *M. annularis* compared to deeper water *M. faveolata* (**Figure 9** and **SI Videos 3** and **4**).

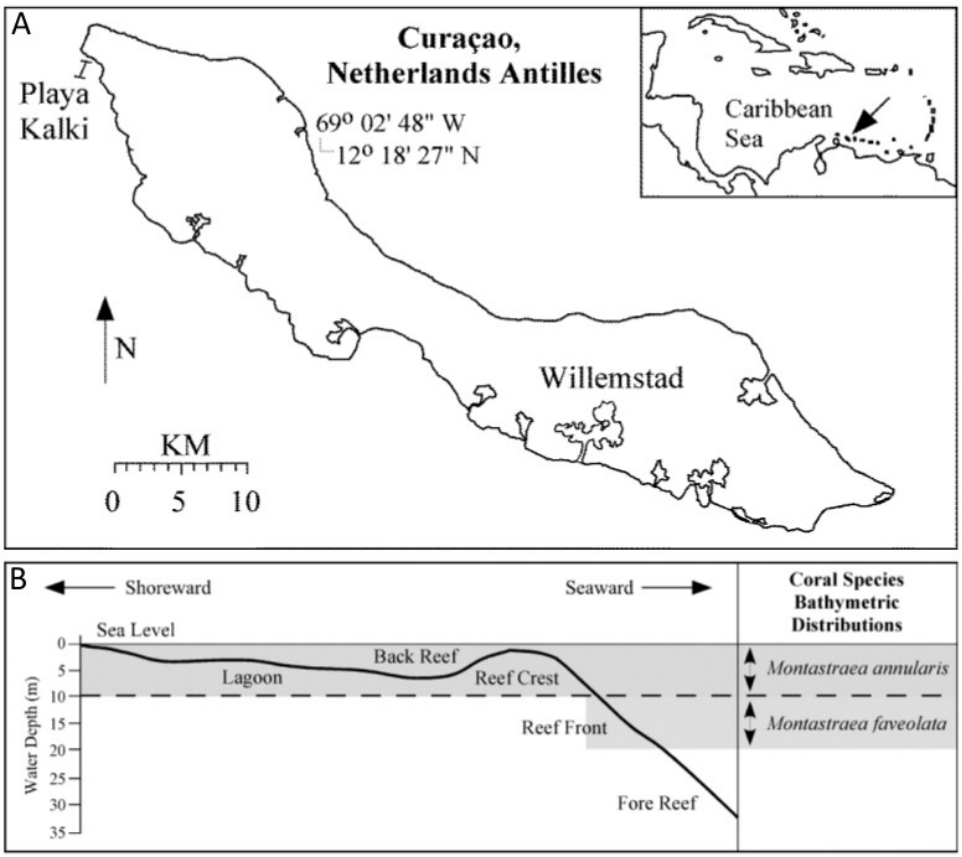

Figure 1. (**A**) **Map of Curaçao in the southern Caribbean Sea**, showing the location of the study site at Playa Kalki on the far northwestern leeward coast of the island. (**B**) Schematic cross-section of the reef-rimmed shelf at Playa Kalki on Curaçao, showing the water depth distributions of *M. annularis* and *M. faveolata*. Please click here to view a larger version of this figure.

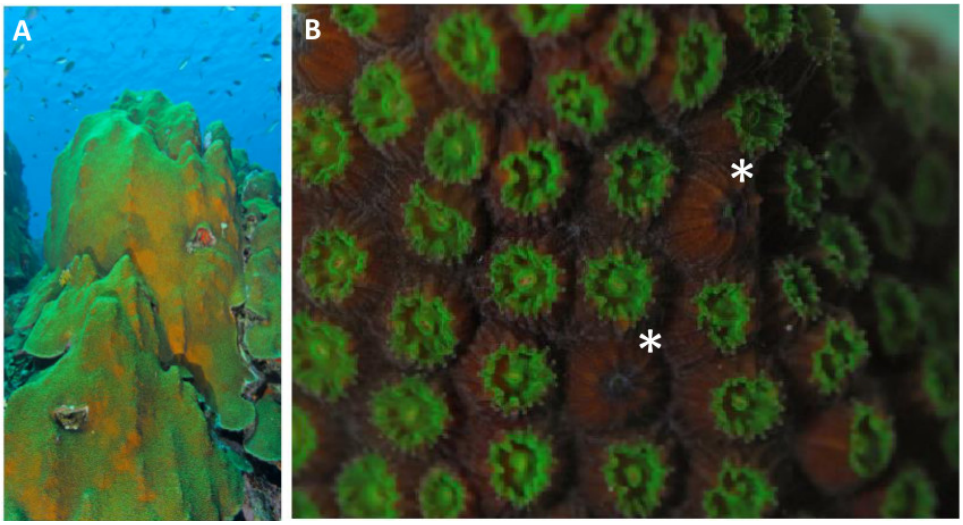

Figure 2. (**A**) ***In situ*** **underwater field photograph at 12 m WD of** ***M. faveolata*** **at Playa Kalki, Curaçao.** (**B**) Close up enlargement of the image in (**A**) showing the individual coral polyps of *M. faveolata* in daytime lighting conditions (each polyp is approximately 2 mm in diameter, some of which are retracted, denoted by *). Please click here to view a larger version of this figure.

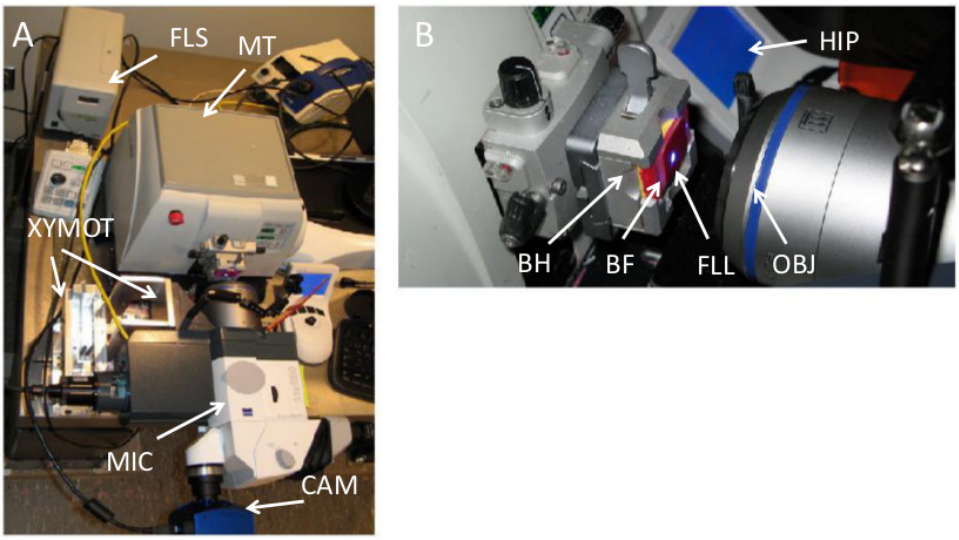

Figure 3. The serial block-face imaging instrumentation. (**A** and **B**) The custom designed microscope holder, holds the Stereolumar microscope at 180° facing the block face of the sample placed in the microtome. When each section was removed, the block face image was captured with the objective and the 2D data was digitally stored. This was done until the sample disappeared in the block. The microscope is moved in x and y direction using a motorized lead screw and the z, adjustment is made to focus the sample. It is important to note that when each 1 µm sample is sectioned, the block moves 1 µm forward, so refocus of the scope is not necessary. XYMOT, Custom built xy translational motorized stage; FLS, Fluorescence light source; MT, Microtome; MIC, Stereomicroscope; CAM, Axiocam monochrome camera; BH, Block holder; BF, Block face of the sample; FLL, Fluorescent light excitation spot on the block face; OBJ, Microscope objective; HIP, Human interface panel. One image at the dimension of 1,388 horizontal x 1,040 vertical pixels in monochrome mode was collected at a xy pixel (single) resolution of 1.25 µm. Please click here to view a larger version of this figure.

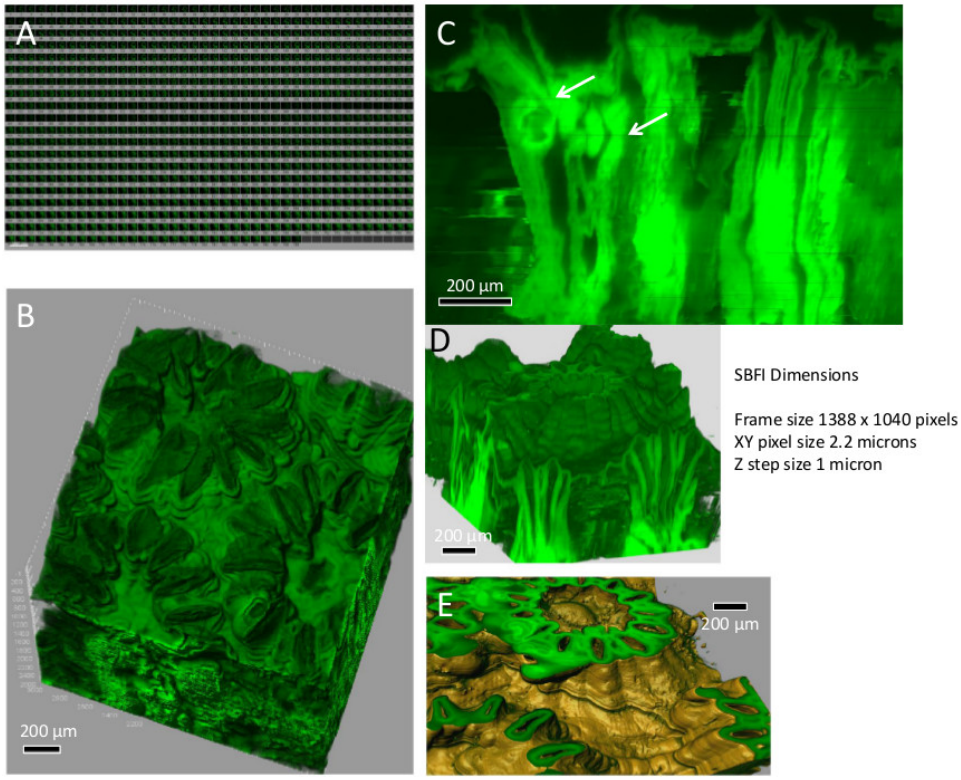

Figure 4. Serial block face imaging of the corals *M. annularis* and *M. faveolata* collected from Playa Kalki, Curaçao. (**A**) Sample data set gallery showing around 800 images of individual 2D images obtained from a polyp at 1 µm resolution in z. (**B**) In another coral sample, the sectioning went well over 2,000 µm in z. The image is showing multiple polyps and compilation of all 2D slices in to a 3D volume under shadow projection using the Imaris volume visualization algorithm. (**C**) Orthogonal projection showing an xz view of the sample in (**B**), one can see the entire depth of the sample over 2 mm and the arrows indicate the black lines where 2D slices were removed due to poor quality; this image is from *M. annularis*. 3D volume (**D**), Isosurface rendering (**E**) and visualization of the SBFI data. (**D**) Multiple coral polyps showing the polyp morphology in longitudinal section on the side and the 3D volume (shadow projection) of a single polyp in the middle. Sectioning and visualization at any angle is possible in 3D (see **SI video**). E. Since voxels are fuzzy in 3D (**D**), the 3D Isosurface rendered surface shows the contour of the coral polyp surface and their contextual arrangement with adjacent polyps (see **SI video**). Please click here to view a larger version of this figure.

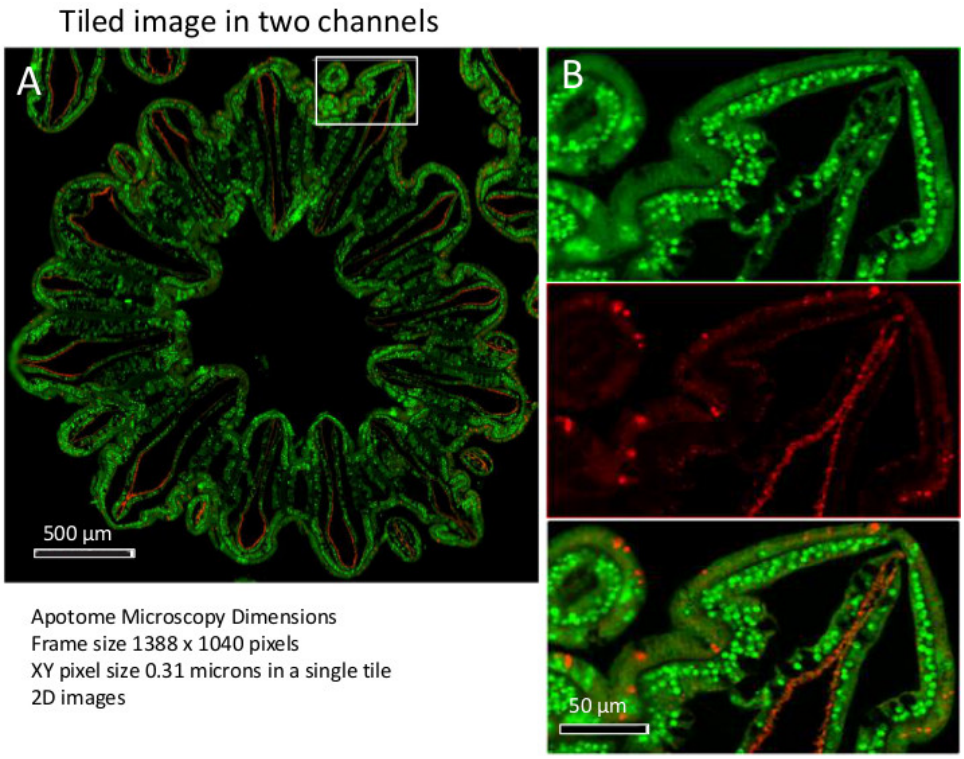

Figure 5. Fluorescence microscopy of coral polyps. (**A**) Cross section of a decalcified polyp of *M. faveolata* exhibiting zooxanthellae with chlorophyll autofluorescence under blue light (shown in green) and mucosal pockets labeled with wheat germ agglutinin (shown in red) as imaged under red light. The image is automatically tiled in two channels and stitched and aligned using the instrument software. (**B**) Enlargement of the box shown in (**A**), showing individual zooxanthellae (each green circles, approximately 6-8 µm in diameter in green) and the surface mucus layer (red), and the merge of both channels. Please click here to view a larger version of this figure.

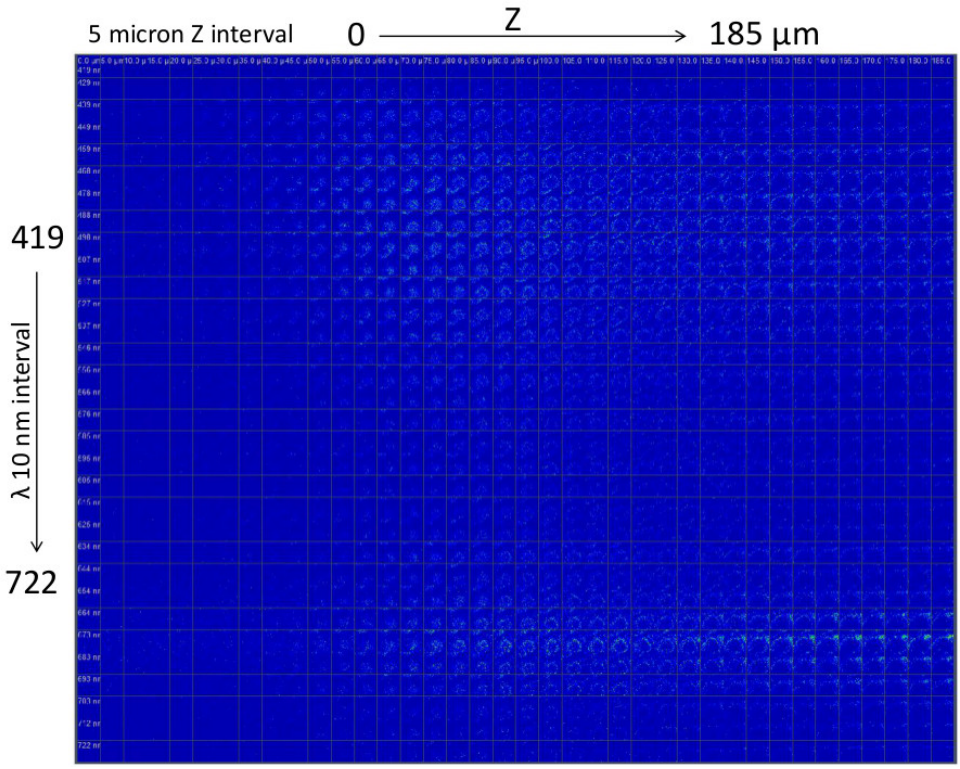

Figure 6. Two-photon spectral characterization of fluorescence from corals. Using the spectral detector of the LSM 710 system, fluorescence signals from the entire visible spectrum (419-722 nm) were scanned over a depth of around 190 µm. The image shows the depth interval at 5 µm in x axis for the z stack and the y axis is wavelength from 419-722 nm acquired at 10 nm interval (a total around 1,154 images showed). One can see the two spectral components, one centered at 500 nm and the second at 650 nm. A two-photon laser excitation wavelength of 780 nm was used to obtain the emission profiles. Please click here to view a larger version of this figure.

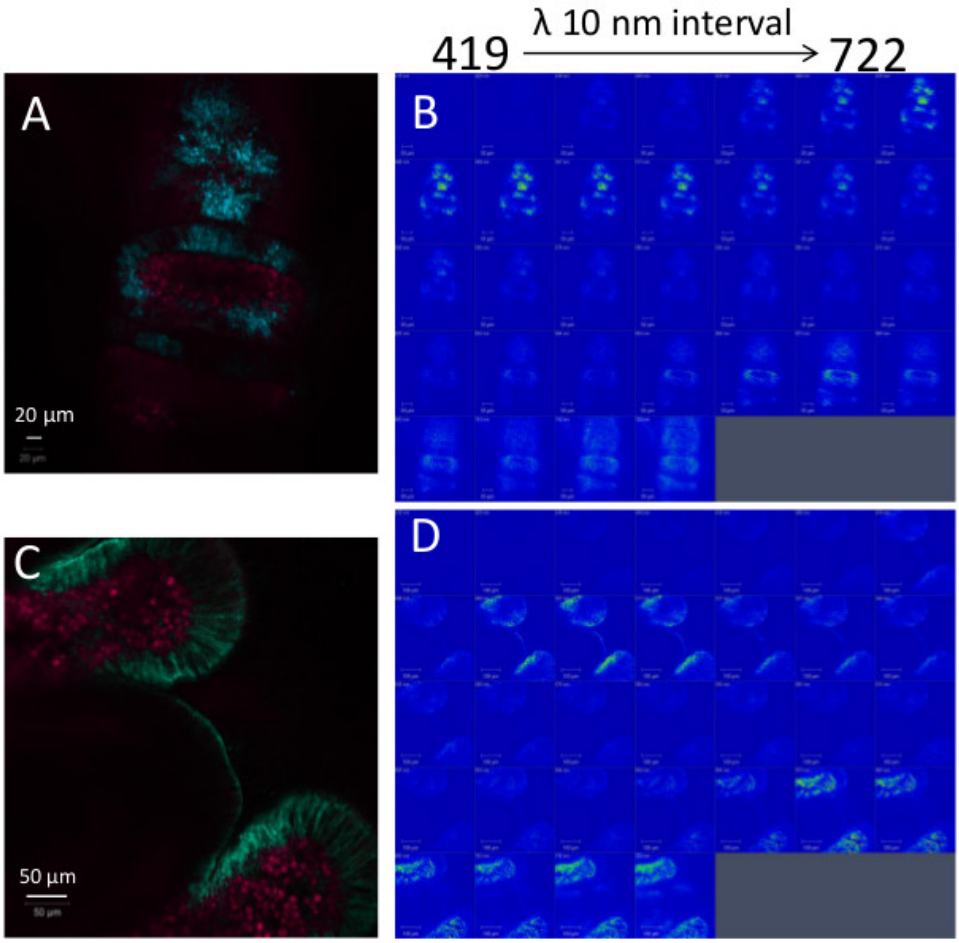

Figure 7. Characterization of the two spectral components. (**A**) The spectral profile of background (blue), autofluorescence from chromatophores (green) and chlorophyll fluorescence (red) excited by the two photon laser excitation wavelength of 780 nm laser. The spectra derived shown at the right side of the multicolor spectral data overlaid and pseudo-colored according to the emission profile. (**B**) The individual spectral bins where the signals are collected at 10 nm interval to derive the spectra and the image in (**A**). Note that the two distinct components, one centered at approximately 500 nm (chromatophore autofluorescence) and the other over 675 nm (chlorophyll fluorescence). Please click here to view a larger version of this figure.

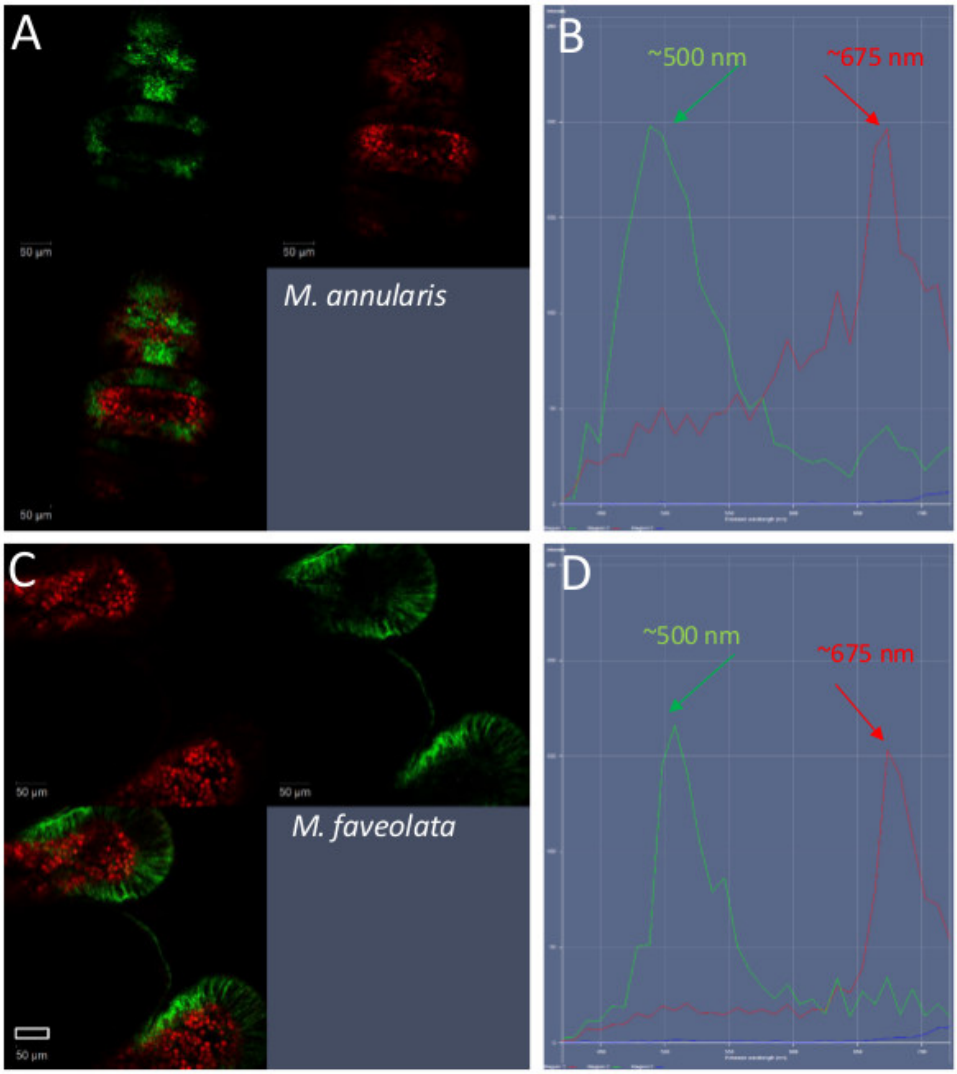

Figure 8. The same images in Figures 7A and 7B, spectral data unmixed using the software and their corresponding emission peaks/ spectra. In both *M. annularis* and *M. faveolata*, the spectral components are very similar, as well their emission peaks. The significant difference, however, is due to the location of these spectral components and their abundance (see **Figure 9**). Please click here to view a larger version of this figure.

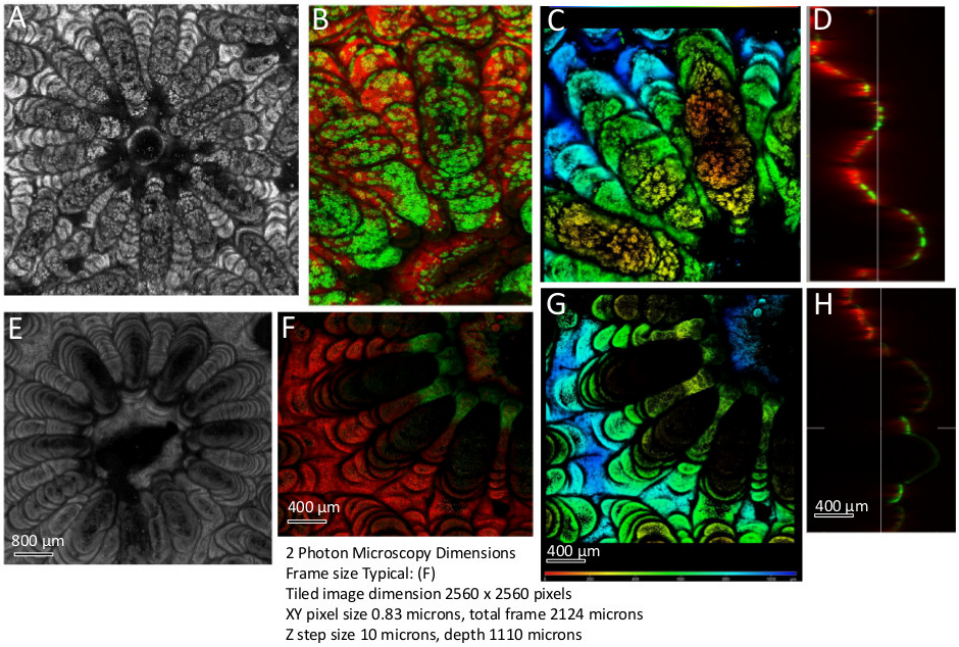

Figure 9. Two-photon fluorescence 3D images of coral polyps from *M. annularis* (A-D) and *M. faveolata* (E-H). (**A** and **E**) were imaged with no spectral separation of components using 780 nm excitation of the two-photon laser, with the optical signal collected from 450-700 nm. (**B** and **F**) were collected with the same excitation (780 nm), but two PMT detectors were used simultaneously to collect the data from two components *i.e.*, one from 500-550 nm (green-chromatophore autofluorescence) and the other 650-720 nm (red-Chlorophyll fluorescence). (**C** and **G**) are depth coded images of (**B** and **F**), red is shallowest and blue is deepest components in 2D. (**D** and **H**) are yz images of cut through (**B** and **F**) respectively, showing the fluorescence is coming only from the surface of the coral and the skeleton does not have any fluorescence at 780 nm excitation. Note the substantial difference in chromatophore content between the two corals. The *M. annularis* habitat (0-10 m WD) is shallower than the *M. faveolata* habitat (10-20 m WD). Please click here to view a larger version of this figure.

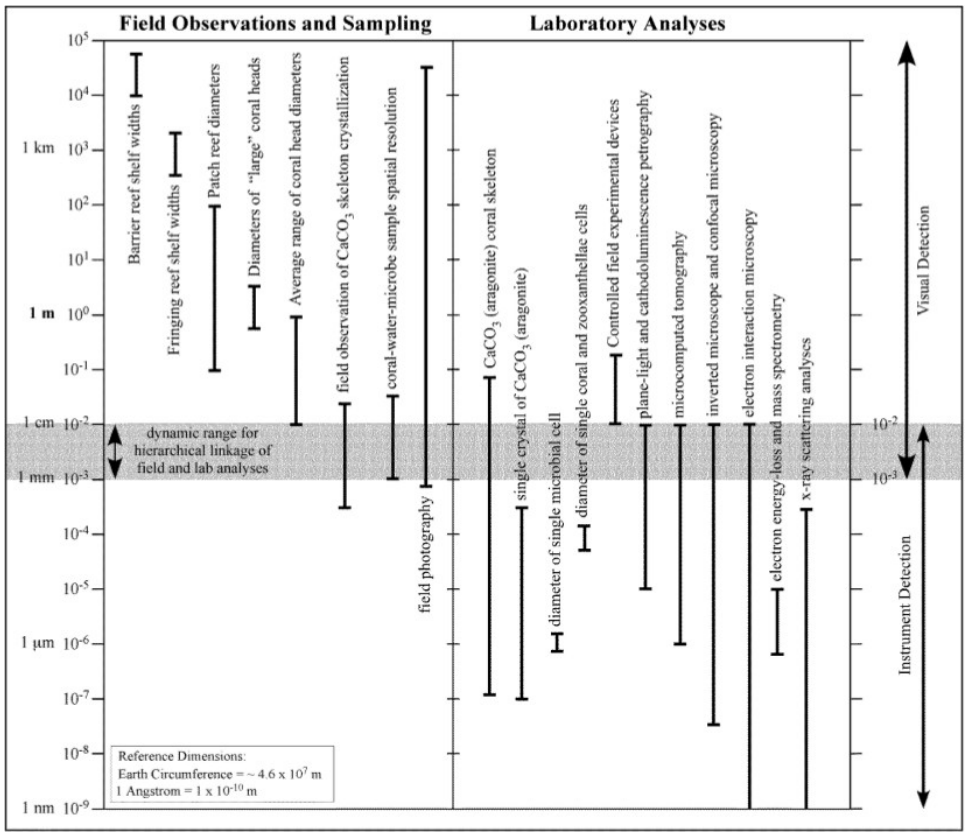

Figure 10. The Powers of Ten hierarchical spatial structure of studies of coral reef ecosystems. Please click here to view a larger version of this figure.

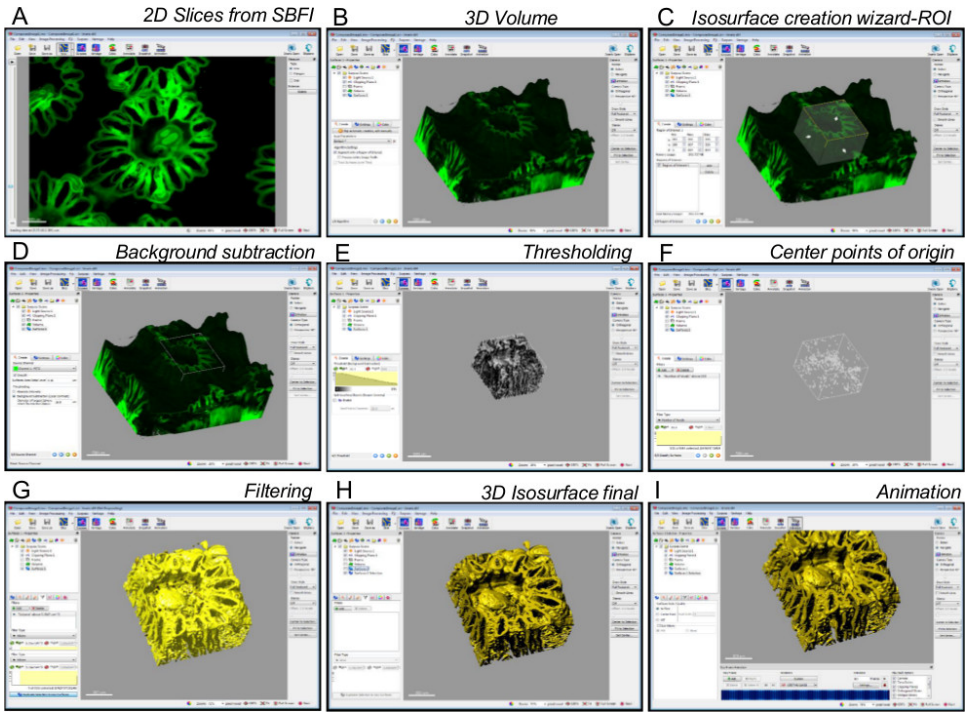

SI Figure 1. Screen shots showing steps (A-I) involved in the creation of 3D volume and isosurface rendering from either the SBFI data or the 2Photon microscopy using the image analysis software (see Materials Table). (**A**) the 2D slices of the raw data in slice mode showing a single plane; (**B**) 3D volume of all the 2D slices; (**C**) the isosurface creation wizard with a region of interest (ROI) selected; (**D**) an algorithm with a background subtraction selected; (**E**) a threshold value applied to pick up the pixels which represent the data; (**F**) center seed points of the surface; (**G**) a volume based filter is applied to eliminate smaller volume of debris and noise; (**H**) the final 3D rendered isosurface; (**I**) key frame animation wizard to create the movies as in the SI videos. The final rendered images are shown in both volume and isosurface modalities in the **SI Videos 3-7**. The protocol steps 3.1.3-3.1.5 covers these procedures. Please click here to view a larger version of this figure.

Material/Equipment	Company	Catalog/Model Number	Comments/Description
Coral Tissue Skeleton	None	None	2.5 cm Biopsy from natural habitat
Arch Punch Coring Device	C.S. Osborne and Company	No. 149	For Coral biopsy collection
Paraformaldehyde	Electron Microscopy Sciences	RT 15700	16% Pre-diluted
Histoclear/Safeclear II	Electron Microscopy Sciences	RT 64111-04	Non-Toxic alternate to Xylene, Dehydration and Deparafinization
Xylene and Ethanol	Fisher Scientific	Fisher Scientific	Dehydration
Paraffin Wax	Richard Allen Scientific	Type H REF 8338	Infiltration solution
Vybar	The Candle Maker	None	Component of Red Wax
Stearin	The Candle Maker	None	Component of Red Wax
Sudan IV	Fisher Chemical	S667-25	Red Wax-Opaque background
Wheat Germ Agglutinin (WGA)	Life Technologies	W32466	For labeling Coral Mucus
Prolong Gold	Life Technologies	P36095	Anti-fade mounting media
Fluoro Dish	World Precision Instruments	FD-35-100	For two-photon imaging
XY Motor, Driver and Controller	Lin Engineering	211-13-01R0, R325, R256-RO	XY Translational Movement
Hot Plate	Corning	DC-220	Melting all wax
Convection Oven	Yamato	DX-600	Infiltration and Embedding
Tissue Processor	Leica	ASP 300	Dehydration, Infiltration
Microtome	Leica	RM2055	Disposable knifes
Stereo Microscope	Carl Zeiss	Stereolumar V 12	1.5x (30 mm WD) Objective
Fluorescence Microscope with ApoTome	Carl Zeiss	Axiovert M 200, ApoTome I System	Imaging thin section of a polyp: Zooxanthellae

Axiocam camera	Carl Zeiss	MRm	Monochrome camera 1388x1040 pixels
Axiovision Software	Carl Zeiss	Version 4.8	Image acquisition program
Two-Photon Laser	Spectraphysics	Maitai eHP, pulsed laser (70 fs)	With DeepSee module
Laser Scanning Microscope	Carl Zeiss	LSM 710 with Spectral Detector	34 channel PMT detection
Zen Software	Carl Zeiss	2010 or above	for two-photon and spectral image acquisition
Imaris Suite Software	Bitplane, Inc.,	Version 7.0 or above	3D Volume, Iso-surface Rendering, Visualization

Table 1. Key materials, equipment, microscopes, and software used in this study.

SI Video 1. *In situ* underwater field video showing the coral habitat at 12 m WD of *M. faveolata* at Playa Kalki, Curaçao.

SI Video 2. Individual 2D serial block face images of the 3D rendered image shown in **Figure 4E**.

SI Video 3. Isosurface 3D rendered serial block face image presented in **Figure 4E** and **SI video 1** showing the topography of the coral polyp.

SI Video 4. 3D volume rendered raw data two-photon microscopy image of the coral polyp *M. faveolata*. The excitation is 780 nm and the emission captured simultaneously at two band widths for zooxanthellae (pseudo-colored red, 600-700 nm) and chromatophores (pseudo-colored green, 500-550 nm).

SI Video 5. 3D volume rendered in Isosurface-spots two-photon microscopy image of the coral polyp *M. faveolata*. The excitation is 780 nm and the emission captured simultaneously at two band widths for zooxanthellae (pseudo-colored red, 600-700 nm) and chromatophores (pseudo-colored green, 500-550 nm).

SI Video 6. 3D volume rendered raw data two-photon microscopy image of the coral polyp *M. annularis*. The excitation is 780 nm and the emission captured simultaneously at two band widths for zooxanthellae (pseudo-colored red, 600-700 nm) and chromatophores (pseudo-colored green, 500-550 nm).

SI Video 7. 3D volume rendered Isosurface-spots two-photon microscopy image of the coral polyp *M. annularis*. The excitation is 780 nm and the emission captured simultaneously at two band widths for zooxanthellae (pseudo-colored red, 600-700 nm) and chromatophores (pseudo-colored green, 500-550 nm).

Discussion

Coral reef research is a highly interdisciplinary research effort, involving analysis of the simultaneous physical, chemical, and biological phenomena that operate in the marine environment. The study of complex coral reef ecosystems is therefore best completed within a 'Powers of Ten' contextual framework (**Figure 10**). This graphic compilation illustrates that the coral ecosystem covers a wide range of spatial dimensions (10^{-9} to 10^{5} m). Furthermore, this exercise illustrates that geobiological analyses at an intermediate length-scale of 1 mm-1 cm are the bridge needed to combine field and laboratory analyses. This Powers of Ten framework is the context for the experiments, analyses, modeling, and synthesis of the physical, chemical, and biological parameters that control Curaçao coral reef ecosystems.

The present study is the first to apply the fully integrated suite of FM, SBFI and CLSM techniques to track the response of apparently healthy corals to increasing water depth. Light microscopy tools available to image whole tissue or thick biological samples have been limited due to a variety of optical constraints posed by the samples themselves, which include absorption, scattering, and other phenomena. Within just the last decade, SBFI scanning electron microscopy was used at ultra-high resolutions[31] as well as light microscopic imaging using wide-field based SBFI imaging of several biological samples. This has included analyses of everything from brain to whole heart tissues and even samples containing bones that were ground, polished, labeled, and imaged at the same time after each section was made[23-29]. Recently, fluorescence and confocal microscopy were used to reveal the contours, shape, and distribution of proteins and pigments in biological samples[32-33]. However, the 3D structure of individual coral polyps had not been previously resolved. The prerequisite for SBFI with coral samples is decalcification, as the calcium carbonate must be removed before rendering the samples amenable to infiltration and sectioning using a regular microtome.

This is where two-photon fluorescence microscopy becomes indispensable for the analysis of biological tissues due to its unique two-photon excitation phenomena. This led to extended depth penetration[33-34]of the coral tissues in the present study, where the decalcification step was effectively eliminated due to the nonlinear two-photon excitation phenomena[34]. In addition, the precompensation module with the two-photon laser provided much shorter pulse width, which additionally improved penetration depth. On the sample side, since calcium carbonate does not absorb the near infrared light at 780 nm, depth penetration is limited typically by the working distance of the objective. Yet another disadvantage of decalcification and the removal of coral skeleton is the loss of structural integrity of the coral tissue, which makes tissue volume estimates even harder after the sample has gone through multiple dehydration and rehydration steps and embedding in water-free wax. This emphasizes the importance of determining coral tissue volumes both before and after processing.

The confocal characterization of fluorescent proteins of coral has been completed for Great Barrier Reef corals and the protective spectral properties have been correlated with depth of the coral habitat[32]. However, in the present study we demonstrate for the first time using two-photon microscopy that there is a substantial reduction of chromatophores everywhere in deep water coral except in mouth tissues. In addition, the distinct changes in the distribution of zooxanthellae with respect to the chromatophores has been observed across depth transects in *M. annularis*, where the shallow-water coral tissues are completely covered with chromatophores. With the resolution provided by the high-magnification imaging (**Figures 8C** and **8D**), we can now precisely quantify the area and volume taken up by the zooxanthellae, and their tissue

density ratios can be determined with respect to other cellular components. Taken together, the integration of SBFI and two-photon fluorescence spectral imaging in the present study have yielded vitally important new insights into the morphology and structure of coral tissues. This data will help to quantify the individual components of coral tissue, either at the individual polyp level or at the contextual level of interplay between colonial polyps on an entire coral head. This context will now permit the adaptive response of the coral holobiont to changes in sea level water depth and irradiance to be quantitative tracked and predicted.

Disclosures

The authors declare no conflict of interests.

Acknowledgements

We thank Donna Epps, histologist at Institute for Genomic Biology, University of Illinois Urbana-Champaign (UIUC), for her capable technical assistance in sample preparation and sectioning. This work was supported by a research grant to B.W. Fouke from the Office of Naval Research (N00014-00-1-0609). In addition, C.A.H. Miller received grants from the UIUC Department of Geology Wanless Fellowship, UIUC Department of Geology Leighton fund and UIUC Department of Geology Roscoe Jackson fieldwork fund. Interpretations presented in this manuscript are those of the authors and may not necessarily represent those of the granting institutions. We also thank the Caribbean Research and Management of Biodiversity (Carmabi) laboratory on Curaçao for their support and collaboration in collecting the coral tissue biopsy samples. We thank Claudia Lutz, IGB Media Communication Specialist for her able language correction.

References

1. Stocker, T.F., D. Qin, G.-K. Plattner, M. Tignor, S.K. Allen, J. Boschung, A. Nauels, Y. Xia, V. Bex and P.M. Midgley (eds.) *Climate Change 2013: The Physical Science Basis. Contribution of Working Group I to the Fifth Assessment Report of the Intergovernmental Panel on Climate Change.* Cambridge University Press, 1535 (2013).
2. Buddemeir, R.W., Kleypas, J.A., and Aronson, R.B. Coral Reefs & Global Climate Change: Potential Contributions of Climate Change to Stresses on Coral Reef Ecosystems. *Pew Center on Global Climate Change.* **46** (2004).
3. Wilkinson, C. *Status of coral Reefs of the world.* Australian Institute of Marine Science, Townsville, 1-2 (2004).
4. Lough, J.M. Climate records from corals. *WIREs Clim. Chang.* **1,** 318-331 (2010).
5. Harvell, C. D., *et al*. Tropical Archaea: diversity associated with the surface microlayer of corals. *Mar. Ecol. Prog. Ser.* **273,** 81-88 (2004).
6. Rosenberg, E., and Loya, Y. Coral Health and Disease. *Springer.* **488** (2004).
7. Rohwer, F., M. Breitbart, J. Jara, F. Azam, and N. Knowlton. Diversity of bacteria associated with the Caribbean coral *Montastrea franksi*. *Coral Reefs.* **20,** 85-91 (2001).
8. Frias-Lopez, J., Zerkle, A.L., Bonheyo, G.T. and Fouke, B.W. Partitioning of bacterial communities between seawater and healthy, black band diseased, and dead coral surfaces. *Appl. Environ. Microbiol.* **68,** 2214-2228 (2002).
9. Stanley Jr, G. D. The evolution of modern corals and their early history. *Earth Sci. Rev.* **60,** 195-225 (2003).
10. Piggot, A.M., Fouke, B.W., Sivaguru, M., Sanford, R., Gaskins, H.R. Change in zooxanthellae and mucocyte tissue density as an adaptive response to environmental stress by the coral *Montastraea annularis*. *Mar. Biol.* **156,** 2379-2389 (2009).
11. Stanley Jr, G. D. Photosymbiosis and the evolution of modern coral reefs. *Evolution.* **1,** 3 (2006).
12. Gordon, B.R., and Leggat, W., 2010. Symbiodinium—Invertebrate Symbioses and the Role of Metabolomics. *Mar. Drugs.* **8**, 2546-2568 (2010).
13. Schlichter, D., Weber, W., Fricke, H.W. A chromatophore system in the hermatypic, deep-water coral *Leptoseris fragilis* (Anthozoa: Hexacorallia). *Mar. Biol.* **89,**143-147 (1994).
14. Fouke, B.W., Meyers, W.J., Hanson, G.N., and Beets, C.J. Chronostratigraphy and dolomitization of the Seroe Domi Formation, Curacao, Netherlands Antilles. *Facies.* **35,** 293-320 (1996).
15. Frias-Lopez, J., Bonheyo, G.T., Jin, Q., and Fouke, B.W. Cyanobacteria associated with coral black band disease in Caribbean and Indo-Pacific reefs. *Appl. Environ. Microbiol.***69,** 2409-2413 (2003).
16. Frias-Lopez, J., Klaus, J., Bonheyo, G.T., and Fouke, B.W. The bacterial community associated with black band disease in corals. *Appl. Environ. Microbiol.* **70,** 5055-5062 (2004).
17. Frias-Lopez, J., Bonheyo, G.T., and Fouke, B.W. Identification of differential gene expression in bacteria associated with coral black band disease using RNA-arbitrarily primed PCR. *Appl. Environ. Microbiol.* **70,** 3687-3694 (2004).
18. Klaus, J.S., Frias-Lopez, J., Bonheyo, G.T., Heikoop, J.M., and Fouke, B.W. Bacterial communities inhabiting the healthy tissues of two Caribbean reef corals: interspecific and spatial variation. *Coral Reefs.* **24,** 129-137 (2005).
19. Klaus, J., Janse, I., Sandford, R., and Fouke, B.W. Coral microbial communities, zooxanthellae, and mucus along gradients of seawater depth and coastal pollution. *Environ. Microbiol.* **9,** 1291-1305 (2007).
20. Duyl, F. C. *Atlas of the living reefs of Curacao and Bonaire (Netherlands Antilles).* Diss. Vrije Universiteit, Amsterdam (1985).
21. Carricart-Ganivet, J.P. Sea surface temperature and the growth of the West Atlantic reef building coral *Montastraea annularis*. *J. Exp. Mar. Biol. Ecol.* **302,** 249-260 (2004).
22. Barnes, D.J. and Lough, J.M. Coral skeletons: Storage and recovery of environmental information. *Global Chang. Biol.* **2,** 569-582 (1996).
23. Mohun, T. J. and Weninger, W. J. Generation of volume data by episcopic three-dimensional imaging of embryos. *Cold Spring Harb. Protoc.* **6**, pdb-prot 069591 (2012).
24. Mohun, T. J. and Weninger, W. J. Imaging heart development using high-resolution episcopic microscopy. *Curr. Opin. Genet. Dev.***21,** 573-578 (2011).
25. Mohun, T. J. and Weninger, W. J. Embedding embryos for episcopic fluorescence image capturing (EFIC). *Cold Spring Harb. Protoc.***6**, pdb-prot069575 (2012).
26. Rosenthal, J. *et al*. Rapid high resolution three dimensional reconstruction of embryos with episcopic fluorescence image capture. *Birth Defects Res. C: Embryo Today: Rev.* **72,** 213-223 (2004).

27. Slyfield, C. R. *et al.* Three#dimensional surface texture visualization of bone tissue through epifluorescence#based serial block face imaging. *J. Microsc.* **236,** 52-59 (2009).
28. Weninger, W. and Mohun, T. Phenotyping transgenic embryos: a rapid 3-D screening method based on episcopic fluorescence image capturing. *Nat. Genet.* **30,** 59-65 (2001).
29. Weninger, W. and Mohun, T. Three-dimensional analysis of molecular signals with episcopic imaging techniques. *Reporter Genes.* Humana Press, 35-46 (2007).
30. Gerneke, D. A. *et al.* Surface imaging microscopy using an ultramiller for large volume 3D reconstruction of wax#and resin#embedded tissues. *Microsc. Res. Tech.***70,** 886-894 (2007).
31. Denk, W. and Horstmann, H. Serial block-face scanning electron microscopy to reconstruct three-dimensional tissue nanostructure. *PLoS Biol.* **2,** e329, (2004).
32. Salih, A., Larkum, A., Cox, G., Kühl, M., Hoegh-Guldberg, O. Fluorescent pigments in corals are photoprotective. *Nature.* **408,** 850-853 (2000).
33. Sivaguru, M., Mander, L., Fried, G., Punyasena, S. W. Capturing the surface texture and shape of pollen: A comparison of microscopy techniques. *PloS one.* **7**(6), (2012).
34. Helmchen F., Denk, W. Deep tissue two-photon microscopy. *Nat. Methods.* **2,** 932-940 (2005).

